*Quantum Electronics* **47** (10) 887–891 (2017) 

*NONLINEAR-OPTICAL PHENOMENA* https://doi.org/10.1070/QEL16511

# Optimisation of spontaneous four-wave mixing in a ring microcavity*

I.N. Chuprina, P.P. An, E.G. Zubkova, V.V. Kovalyuk, A.A. Kalachev, G.N. Gol'tsman

***Abstract.*** **A theory of spontaneous four-wave mixing in a ring microcavity is developed. The rate of emission of biphotons for pulsed and monochromatic pumping with allowance for the dispersion of group velocities is analytically calculated. In the first case, pulses in the form of an increasing exponential are considered, which are optimal for excitation of an individual resonator mode. The behaviour of the group velocity dispersion as a function of the width and height of the waveguide is studied for a specific case of a ring microcavity made of silicon nitride. The results of the numerical calculation are in good agreement with the experimental data. The ring microcavity is made of two types of waveguides: completely etched and half etched. It is found that the latter allow for better control over the parameters in the manufacturing process, making them more predictable.**

***Keywords:*** *spontaneous four-wave mixing, ring microcavity, silicon nitride.*

## 1. Introduction

The development of integrated sources of single-photon and entangled two-photon states of light is an important issue of quantum optics and quantum informatics [1, 2]. One promising approach to designing such sources is to use nonlinear optical effects in CMOS-compatible materials, such as silicon nitride [3]. In particular, spontaneous four-wave mixing (SFWM) in a microcavity allows one to combine a number of useful properties in one device [4–10]. First, the rate of the nonlinear process can be substantially increased due to the small volume of modes and high finesse of the resonator, which allows the requirements to the pump power to be lowered [4, 6, 10], while an increase in the dispersion region in small resonators makes it possible to facilitate frequency demultiplexing and pump field filtering [9]. Second, an increase in the rate of generation of photon pairs by means of a resonator simultaneously reduces their spectral width [8], making quantum states of light more suitable for recording in quantum memory devices. Third, the CMOS-compatible manufacturing process and high material stability allow one to embed sources into scalable photonic integrated circuits [9] and to approach the deterministic emission of single photons using spatial multiplexing [11]. Compared with the integred sources based on spontaneous parametric down-conversion, in the case of SFWM all optical wavelengths are in a relatively narrow range near the telecommunication wavelength, which simplifies the development of integrated optical elements and the phase matching of the interacting waves.

The SFWM theory in ring microcavities was developed in a number of papers [10, 12–19]. In this case, the monochromatic pumping was usually considered, which is often used in experiments, but is not suitable for multiplexing and fabricating scalable optical circuits. In the case of pulsed pumping, the authors of Refs [12, 19] showed that using short and broadband pump pulses, it is possible to reduce the frequency correlations between the emitted photons or even completely eliminate them, which is critical for the conditional preparation of pure single-photon states. In addition, as shown by Vernon et al. [18], the critical coupling, usually used in the case of continuous pumping, is not optimal from the point of view of the efficiency of the conditional preparation of photons. To achieve high efficiency, it is necessary to use an overcoupled resonator. However, in this case, the generation rate for a given input power of the pump is reduced. In this paper, we analyse SFWM, considering pulses in the form of an increasing exponential, which are optimal for the excitation of a single-mode resonator at any ratio of radiative and non-radiative losses.

## 2. Model and basic equations

The SFWM process involves the action of a laser pump beam on a nonlinear material characterised by third-order nonlinearity in the electric field, $\chi^{(3)}$. The nonlinear interaction inside a crystal leads to the annihilation of two photons in the pump modes at random time instants and to the creation of two photons, usually called signal and idler photons, in other modes of the electromagnetic field. In this paper we consider a single-port racetrack microring resonator (Fig. 1), characterised by finesse

$$F = \frac{\pi\sqrt{\tau a}}{1 - \tau a}, \quad (1)$$

*Presented at the Russian–British Symposium on Quantum Technologies (Moscow, 20–23 March 2017)

**I.N. Chuprina, A.A. Kalachev** Kazan E.K. Zavoisky Physical-Technical Institute, Kazan Scientific Center, Russian Academy of Sciences, ul. Sibirskii trakt 10/7, 420029 Kazan, Russia; Kazan Federal University, ul. Kremlevskaya 18, 420008 Kazan, Russia; e-mail: a.a.kalachev@mail.ru;
**P.P. An, E.G. Zubkova, V.V. Kovalyuk, G.N. Gol'tsman** Kazan E.K. Zavoisky Physical-Technical Institute, Kazan Scientific Center, Russian Academy of Sciences, ul. Sibirskii trakt 10/7, 420029 Kazan, Russia; Moscow State Pedagogical University, ul. Malaya Pirogovskaya 1, Str. 1, 119991 Moscow, Russia

Received 19 September 2017
*Kvantovaya Elektronika* **47** (10) 887–891 (2017)
Translated by I.A. Ulitkin

where $\tau$ is the self-coupling coefficient and $a$ is the transmission amplitude per round trip, and the rate of field decay is

$$\kappa = \frac{2\pi c}{L n_g}\frac{1}{F}, \tag{2}$$

where $L$ is the resonator length and $n_{\mathrm{g}}$ is the group refractive index.

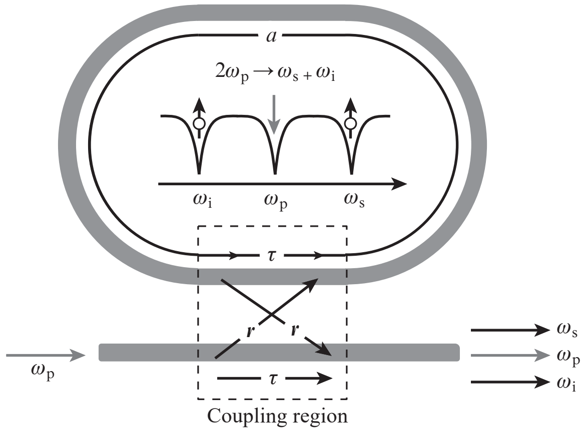


**Figure 1.** Scheme of a nonlinear racetrack microring resonator connected with a waveguide (bus). The coefficients $r$ and $\tau$ are the cross-coupling and self-coupling probability amplitudes ($|r|^2 + |\tau|^2 = 1$), the coefficient $a$ is the transmission amplitude of the ring resonator per one round trip.

The created two-photon states can be calculated within the framework of the first-order perturbation SFWM theory in an optical waveguide or fibre (see, for example, Ref. [20]), modified taking into account the input–output formalism for open cavities [21]. This approach was used for the analysis of SFWM in a resonator in Refs [13, 22].

For simplicity, we consider a degenerate pump scheme. It is assumed that the pump field corresponds to the resonator mode in the zero-dispersion region of the ring microcavity. In this case, the signal and idler photons are emitted into the adjacent modes of the resonator (Fig. 1), which are separated from the pump mode, in general, by different frequency intervals due to the dispersion of the group velocities. Since we are interested in an over-coupled resonator, we can put $a = 1$.

Spontaneous four-wave mixing in a resonator is described by the effective Hamiltonian:

$$H(t) = \frac{3\varepsilon_0}{4}\int \mathrm{d}\boldsymbol{r}\,\chi^{(3)}(\boldsymbol{r})E_{\mathrm{s}}^{(-)}(\boldsymbol{r},t)E_{\mathrm{i}}^{(-)}(\boldsymbol{r},t)$$

$$\times E_{\mathrm{p}}^{(+)}(\boldsymbol{r},t)E_{\mathrm{p}}^{(+)}(\boldsymbol{r},t)\exp(\mathrm{i}\Phi_{\mathrm{NL}}) + \mathrm{H.c.} \tag{3}$$

Here, the positive and negative-frequency parts of the electric field operator have the form

$$E_v^{(+)}(\boldsymbol{r},t) = \mathrm{i}\sqrt{\frac{\hbar\omega_{v0}}{2\varepsilon_0 n_{v0} n_{\mathrm{g}v0}}}\frac{u_v(x,y)}{\sqrt{L}}$$

$$\times\int\frac{\mathrm{d}\omega}{\sqrt{2\pi}}a_v(\omega)\exp(\mathrm{i}\beta_v z - \mathrm{i}\omega t), \tag{4}$$

$$E_v^{(-)} = [E_v^{(+)}]^{\dagger},$$

where $v$ = s, i, p is the mode index; $\beta_v(\omega) = \omega n_v(\omega)/c$ is the propagation constant; $n_v(\omega)$ is the effective refractive index; $\omega_{v0}$ is the centre field frequency corresponding to the resonator mode; $n_{v0} = n_v(\omega_{v0})$; $n_{\mathrm{g}v}(\omega) = c(\mathrm{d}\beta_v/\mathrm{d}\omega)$ is the group refractive index of the mode; $n_{\mathrm{g}v0} = n_{\mathrm{g}v}(\omega_{v0})$; $u_v(x, y)$ is the mode function describing the transverse spatial distribution of the field and normalised $\int|u(x,y)|^2\mathrm{d}x\mathrm{d}y = 1$; and $\Phi_{\mathrm{NL}}$ is the nonlinear contribution of self-modulation and cross-modulation [23].

The annihilation operators of photons in resonator modes, $a_v(\omega)$, and in free-field modes, $a_{v,\mathrm{in}}(\omega)$, $a_{v,\mathrm{out}}(\omega)$, are related by the expressions:

$$a_v(\omega) = \frac{-\mathrm{i}\sqrt{\kappa_v}}{\kappa_v/2 - \mathrm{i}(\omega - \omega_{v0})}a_{v,\mathrm{in}}(\omega) \equiv B_v(\omega)a_{v,\mathrm{in}}(\omega), \tag{5}$$

$$a_v(\omega) = \frac{-\mathrm{i}\sqrt{\kappa_v}}{-\kappa_v/2 - \mathrm{i}(\omega - \omega_{v0})}a_{v,\mathrm{out}}(\omega) \equiv B_v^*(\omega)a_{v,\mathrm{out}}(\omega). \tag{6}$$

For simplicity, we assume that $\kappa_{\mathrm{s}} = \kappa_{\mathrm{i}} = \kappa_{\mathrm{p}} = \kappa$ and an analogous relation holds for the finesse of the resonator, $F_v$.

The state vector of the SFWM field in the first order of perturbation theory is calculated from the formula

$$|\psi\rangle = |0\rangle|\alpha\rangle - \frac{i}{\hbar}\int_{-\infty}^{+\infty}\mathrm{d}t\,H(t)|0\rangle|\alpha\rangle = |0\rangle|\alpha\rangle + |\psi_2\rangle|\alpha\rangle, \tag{7}$$

where $|0\rangle \equiv |0_{\mathrm{s}}\rangle|0_{\mathrm{i}}\rangle$ is the vacuum state of the signal and idler fields; and $|\alpha\rangle$ is the coherent state of the pump field with a complex amplitude $\alpha$. Since the pump is assumed to be classical, we can replace the $\sqrt{\hbar\omega_{\mathrm{p}0}}\,\alpha(\omega)$ by $\sqrt{W}\,\alpha_{\mathrm{p}}(\omega)$, where $W$ is the pump pulse energy and $\int|\alpha_{\mathrm{p}}(\omega)|^2\mathrm{d}\omega = 1$. Substituting (3)–(6) into formula (7), we obtain

$$|\psi_2\rangle = -\mathrm{i}\gamma L W\sqrt{\frac{\omega_{\mathrm{s}0}\omega_{\mathrm{i}0}n_{\mathrm{p}0}^2}{\omega_{\mathrm{p}0}^2 n_{\mathrm{s}0}n_{\mathrm{i}0}}}\frac{1}{8\pi}\left(\frac{F\kappa}{2\pi}\right)^2$$

$$\times\iint\mathrm{d}\omega_{\mathrm{s}}\mathrm{d}\omega_{\mathrm{i}}B_{\mathrm{s}}(\omega_{\mathrm{s}})B_{\mathrm{i}}(\omega_{\mathrm{i}})I_{\mathrm{p}}(\omega_{\mathrm{s}},\omega_{\mathrm{i}})$$

$$\times h(\Delta\beta)a_{\mathrm{out}}^{\dagger}(\omega_{\mathrm{s}})a_{\mathrm{out}}^{\dagger}(\omega_{\mathrm{i}})|0\rangle, \tag{8}$$

where

$$I_{\mathrm{p}}(\omega_{\mathrm{s}},\omega_{\mathrm{i}}) = \int\mathrm{d}\omega_{\mathrm{p}}B_{\mathrm{p}}(\omega_{\mathrm{p}})B_{\mathrm{p}}(\omega_{\mathrm{s}} + \omega_{\mathrm{i}} - \omega_{\mathrm{p}})$$

$$\times\alpha_{\mathrm{p}}(\omega_{\mathrm{p}})\alpha_{\mathrm{p}}(\omega_{\mathrm{s}} + \omega_{\mathrm{i}} - \omega_{\mathrm{p}}) \tag{9}$$

is the convolution of the spectral amplitude of the pump field in the resonator;

$$\gamma = \frac{3\chi^{(3)}\omega_{\mathrm{p}0}}{4\varepsilon_0 c^2 n_{\mathrm{p}0}^2 A_{\mathrm{eff}}} \tag{10}$$

is the effective nonlinearity, corresponding to SFWM;

$$A_{\mathrm{eff}} = \frac{1}{\iint\mathrm{d}x\mathrm{d}y\,u_{\mathrm{p}}(x,y)u_{\mathrm{p}}(x,y)u_{\mathrm{s}}^*(x,y)u_{\mathrm{i}}^*(x,y)} \tag{11}$$

is the effective area of interaction;

$$h(\Delta\beta) = \frac{1}{L}\int_{-L}^{0} \exp(\mathrm{i}\Delta\beta z)\mathrm{d}z = \mathrm{sinc}(\Delta\beta L/2)\exp(\mathrm{i}\Delta\beta L/2) \quad (12)$$

is the phase-matching function; and

$$\Delta\beta = \beta(\omega_p) + \beta(\omega_s + \omega_i - \omega_p) - \beta(\omega_s) - \beta(\omega_i) + \Phi_{NL} \quad (13)$$

is the phase mismatching. Next, we consider the pump power, for which the value of $\Phi_{NL}$ can be neglected.

Knowing the state vector of the biphoton field (8), it is possible to calculate the number of pairs of photons generated per one pump pulse

$$N = \int\int \mathrm{d}\omega_s \mathrm{d}\omega_i |\langle 0 | a_{out}(\omega_s) a_{out}(\omega_i) | \psi_2 \rangle|^2, \quad (14)$$

which gives

$$N = \frac{1}{(8\pi)^2}\frac{\omega_{s0}\omega_{i0}}{\omega_{p0}^2}\frac{n_{p0}^2}{n_{s0}n_{i0}}\left(\frac{F\kappa}{2\pi}\right)^4 (\gamma L W)^2 \mathrm{sinc}^2(\Delta\beta_0 L/2)$$

$$\times \int\int d\omega_s d\omega_i | B_s(\omega_s) B_i(\omega_i) I_p(\omega_s, \omega_i)|^2. \quad (15)$$

Here it is taken into account that the function $|h(\Delta\beta)|^2$ is a slowly varying function within the profile of the resonator line and can be taken outside the integral sign in the form $\mathrm{sinc}^2(\Delta\beta_0 L/2)$, where $\Delta\beta_0 = 2\beta(\omega_{p0}) - \beta(\omega_{s0}) - \beta(\omega_{i0})$. The remaining integral can be calculated analytically for certain forms of the pump pulse, which are discussed in the next section.

## 3. Pulses in the form of an increasing exponential

Let us consider the pump pulse in the form of an increasing exponential

$$\alpha_p(\omega) = \frac{1}{\sqrt{2\pi}}\frac{-\sqrt{\epsilon}}{(-\epsilon/2) - \mathrm{i}(\omega - \omega_{p0})}. \quad (16)$$

If $\epsilon = \kappa$, then the pulse is optimal for excitation of the resonator mode with the decay rate $\kappa$. In this case, the pump-field spectrum inside the resonator, which is described by the function $B_p(\omega_p)\alpha_p(\omega_p)$ in convolution (9), becomes a Lorentzian and corresponds to an excitation pulse in the form of a two-sided exponent having a maximum value for a given input field energy. For the optimal pump pulse, the convolution function takes the form

$$I_p(\omega_s, \omega_i) = -\frac{2\kappa}{(2\omega_{p0} - \omega_s - \omega_i)^2 + \kappa^2}, \quad (17)$$

and the integral in equation (15) can be written as

$$\int\int \mathrm{d}\omega_s \mathrm{d}\omega_i | B_s(\omega_s) B_i(\omega_i) I_p(\omega_s, \omega_i)|^2 = \frac{3}{2}\frac{(2\pi)^2}{\kappa^2} G(\Delta), \quad (18)$$

where

$$G(\Delta) = \frac{2}{3}\frac{\kappa^2}{(2\pi)^2}\int\int \mathrm{d}\nu_s \mathrm{d}\nu_i \frac{\kappa}{\nu_s^2 + (\kappa/2)^2}$$

$$\times \frac{\kappa}{\nu_i^2 + (\kappa/2)^2}\frac{4\kappa^2}{[(\nu_s + \nu_i + \Delta)^2 + \kappa^2]^2} \approx \left[1 + \frac{1}{2}\left(\frac{\Delta}{\kappa}\right)^2\right]^{-1}. \quad (19)$$

Here, $\Delta$ is the frequency detuning between two modes corresponding to the signal and idler photons, which is due to the group velocity dispersion. If the signal and idler modes are on the same side of the wavelength corresponding to the zero group velocity dispersion, then the frequency detuning takes the form $\Delta = -\beta_2/\beta_1(\Delta_{FSR} m)^2$, where $\beta_1 = n_g/c$; $\beta_2 = -[\lambda^2/(2\pi c)^2] \times \mathrm{d}n_g/\mathrm{d}\lambda$; $\Delta_{FSR} = 2\pi c/(L n_g)$; and $m$ is the number of dispersion regions between the pump mode and the signal (or idler) mode. Assuming that the dispersion is small, and considering modes of the same type, we can put $\forall \nu$, $n_{g\nu 0} = n_g$. Finally, after multiplying the number of emitted pairs of photons by the repetition rate of the pump pulses $R$, we arrive at the following emission rate of photon pairs:

$$N_{puls} = 2^{-8}(\gamma L P_{av})^2 \frac{3\kappa^2}{2R} G(\Delta)$$

$$\times \frac{\omega_{s0}\omega_{i0}}{\omega_{p0}^2}\frac{n_{p0}^2}{n_{s0}n_{i0}}\left(\frac{F}{\pi}\right)^4 \mathrm{sinc}^2\frac{\Delta\beta_0 L}{2}, \quad (20)$$

where $P_{av} = WR$ is the average pump power.

## 4. Regime of monochromatic pumping

Let us now consider SFWM in the case of cw pumping. It can be shown that with $\epsilon \to 0$ in equation (9) and relations

$$\lim_{\epsilon \to 0} |\alpha_p(\omega_p)|^2 = \delta(\omega_p - \omega_{p0}), \quad (21)$$

$$\int \mathrm{d}x\, \delta(\xi - x)\delta(x - \eta) = \delta(\xi - \eta), \quad (22)$$

we obtain the convolution integral

$$I_p(\omega_s, \omega_i) = \frac{2\pi\epsilon}{\kappa}\delta(\omega_s + \omega_i - 2\omega_{p0}), \quad (23)$$

so that the integral in (15) takes the form

$$\int\int d\omega_s d\omega_i | B_s(\omega_s) B_i(\omega_i) I_p(\omega_s, \omega_i)|^2 = 2\epsilon\frac{(2\pi)^2}{\kappa^2} G'(\Delta), \quad (24)$$

where

$$G'(\Delta) = \left[1 + \left(\frac{\Delta}{\kappa}\right)^2\right]^{-1}. \quad (25)$$

Next, by determining the cw pump power $P_{cw}$ as the peak power of the pulse in the limit of infinite duration, $P_{cw} = \lim_{\epsilon \to 0}(W\epsilon)$, we arrive at the emission rate of photon pairs:

$$N_{cw} = 2^{-8}(2\kappa) G'(\Delta)\frac{\omega_{s0}\omega_{i0}}{\omega_{p0}^2}\frac{n_{p0}^2}{n_{s0}n_{i0}}\left(\frac{F}{\pi}\right)^4$$

$$\times (\gamma L P_{cw})^2 \mathrm{sinc}^2(\Delta\beta_0 L/2). \quad (26)$$

Equations (19) and (25) give approximately the same generation rate when $P_{av} = P_{cw}$ and the pulse repetition rate $R$ is close to the decay rate $\kappa$. However, when $R$ decreases, the process of generating photon pairs in the case of the pulsed regime becomes more effective at the same average power of the pump field. In addition, comparing $G(\Delta)$ and $G'(\Delta)$, we can draw a conclusion that the SFWM rate in the monochromatic pulsed regime is more sensitive to the group velocity dispersion than in the case of the pulsed pump regime, as is expected.

## 5. Issues of experimental implementation

Let us consider a ring microcavity formed by a silicon nitride waveguide ($Si_3N_4/SiO_2$). Waveguides made of this material form a promising CMOS-compatible platform for applications of integrated photonics [3]. In particular, Gondarenko et al. [24] demonstrated ring microresonators made of silicon nitride with a finesse exceeding $10^3$ in the telecommunication C-band of wavelengths. To obtain a zero-dispersion wavelength in this range, the waveguide must be sufficiently thick [25]. In this paper, a numerical simulation of the group velocity dispersion $D \equiv (-\lambda/c)\,\mathrm{d}^2n/\mathrm{d}\lambda^2$, analogous to that carried out in Ref. [25], was performed, but we consider a microcavity formed of two straight and two semicircular waveguides (see Fig. 1). The numerical simulation was performed using a commercial program based on the FDTD method (Lumerical Mode Solutions). The Sellmeier formulas for silicon nitride and silicon dioxide were taken from [26] and [27], respectively.

When a zero group velocity dispersion is reached, nondegenerate SFWM becomes possible, which allows frequency-entangled biphoton states to be generated and frequency-division multiplexing of photons to be simplified. In accordance with the numerical calculation (Fig. 2), a waveguide with a height of approximately 500 nm is needed to realise this regime. To verify this conclusion, two ring microcavities with the same total length, the same waveguide width (1 μm), but with different heights (330 and 450 nm) were fabricated on commercially available silicon substrates. The manufacturing process included the stages of photo and electronic lithography.

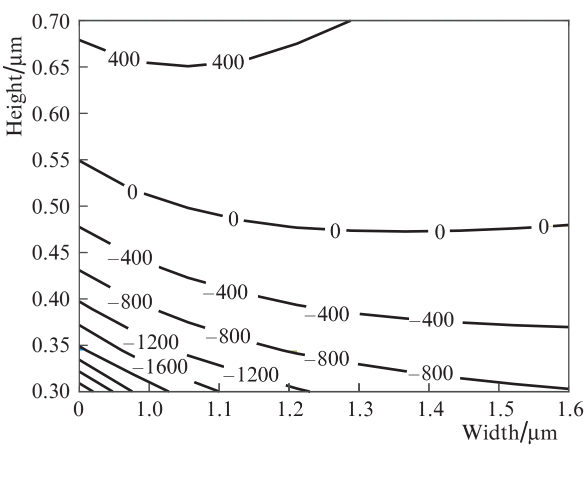


**Figure 2.** Calculated dependence of the group velocity dispersion $D$ on the width and height of the waveguide for the fundamental TE mode at a wavelength of 1550 nm. The racetrack microring resonator has a length of 360 μm and contains two semicircles with a radius of 31 μm. The numbers at the curves are the values of $D$ in ps km$^{-1}$ nm$^{-1}$.

At the first stage, alignment marks were made with the help of positive AZ1512 photoresist. Using thermal evaporation, we sputtered about 5 nm of titanium as an adhesive layer and 200 nm of gold. To finalise the alignment marks, use was made of a list-off in acetone. At the second stage, waveguide structures were transferred to the $Si_3N_4$ layer by electron lithography to a ZEP 520A high-resolution resist and subsequent reactive ion etching using Ar + $CHF_3$ plasma. The residual resist was then removed by plasma purification with oxygen.

To couple radiation from single-mode fibre into a ring microcavity, we used focusing devices based on diffraction gratings [28], optimised for a wavelength of 1550 nm. The coupling loss did not exceed –10 dB. The transmission spectrum was measured by an FRL15DC temperature-tunable distributed-feedback laser module (Fitel) and an HP 70950A optical spectrum analyser. The calculated dispersion parameters $D$ for waveguides of height 330 and 450 nm turned out to be equal to –1600 and –400 ps km$^{-1}$ nm$^{-1}$, respectively. From the obtained data, it is possible to estimate the difference in the values of two adjacent regions of free dispersion, which amounted to 0.03 and 0.007 nm. The corresponding experimental values of 0.05 and 0.01 nm confirm the approximation to zero dispersion with increasing waveguide height.

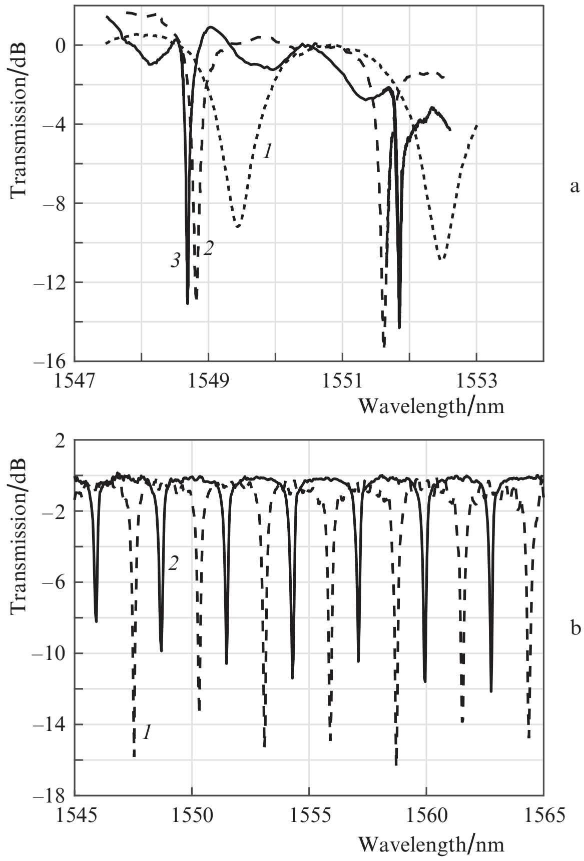


**Figure 3.** Transmission spectra of racetrack microring resonators as a function of the wavelength: (a) with a gap between the bus and the ring (*1*) 0.75, (*2*) 1.0 and (*3*) 1.4 μm for coupling lengths of 80, 100 and 80 μm, respectively (the first resonator is made of a fully etched waveguide, the remaining two are made of a half-etched waveguide); (b) transmission spectra for a half-etched ring microcavity at a gap of (*1*) 0.6 and (*2*) 1.4 μm (coupling length of 120 μm). In both cases, the waveguides had a height of 0.45 μm and a width of 1 μm, the total resonator length was 380 μm.

As an example, let us consider a waveguide with a height of 500 nm and a width of 1050 nm. In this case, the effective interaction area $A_{\rm eff}$ is 0.5 μm$^2$ and, assuming $n_2 = 2.4 \times 10^{-19}$ m$^2$ W$^{-1}$ [29], we obtain an effective nonlinearity $\gamma$ = 3.7 m$^{-1}$ W$^{-1}$. Then, assuming $F$ = 100, $L$ = 100 μm and the cw pump power $P_{\rm cw}$ = 10 mW, we obtain the creation rate of photon pairs, $\sim 10^4$ s$^{-1}$.

Figure 3 shows the transmission spectra of a racetrack microring resonator of the same length (380 μm), but with different gaps and lengths of the coupling region. The increase in the gap, as expected, leads to an increase in the $Q$-factor, so that at a gap of 1.4 μm and a coupling region of 80 μm in length, we obtain a $Q$-factor of 13000. Thus, we have fabricated resonators with two types of waveguides – completely etched and half-etched. We have found that the latter allow a better control over parameters during the manufacturing process, making it more predictable.

## 6. Conclusions

Thus, we have studied spontaneous four-wave mixing in a dielectric ring resonator. An analytical expression is obtained for the rate of emission of photon pairs with cw and pulsed pumping. In the second case, exponential pulses are considered, which are optimal for the excitation of a single-mode resonator. In the particular case of silicon nitride waveguides, it is shown that the zero-dispersion region of the group velocity can be in the telecommunication C-band at suitable values of the width and height of the waveguide. Under such conditions, nondegenerate SFWM becomes possible, which allows one to create frequency-entangled biphoton states and direct outgoing photons to different spatial channels. Ring microresonators made of silicon nitride with different waveguide widths and heights are fabricated and it is shown that, at an optimum waveguide height, the dispersion of group velocities decreases.

***Acknowledgements.*** The work was supported by the Russian Science Foundation (Grant No. 16-12-00045).

## References


1. O'Brien J.L., Furusawa A., Vučković J. *Nature Photon.*, **3**, 687 (2009).
2. Tanzilli S., Martin A., Kaiser F., De Micheli M.P., Alibart O., Ostrowsky D.B. *Laser Photon. Rev*., **6**, 115 (2012).
3. Moss D.J., Morandotti R., Gaeta A.L., Lipson M. *Nature Photon.*, **7**, 597 (2013).
4. Turner A.C., Foster M.A., Gaeta A.L., Lipson M. *Opt. Express*, **16**, 4881 (2008).
5. Clemmen S., Huy K.P., Bogaerts W., Baets R.G., Emplit P., Massar S. *Opt. Express*, **17**, 16558 (2009).
6. Azzini S., Grassani D., Strain M.J., Sorel M., Helt L.G., Sipe J.E., Liscidini M., Galli M., Bajoni D. *Opt. Express*, **20**, 23100 (2012).
7. Engin E., Bonneau D., Natarajan C.M., Clark A.S., Tanner M.G., Hadfield R.H., Dorenbos S.N., Zwiller V., Ohira K., Suzuki N., Yoshida H., Iizuka N., Ezaki M., O'Brien J.L., Thompson M.G. *Opt. Express*, **21**, 27826 (2013).
8. Reimer C., Caspani L., Clerici M., Ferrera M., Kues M., Peccianti M., Pasquazi A., Razzari L., Little B.E., Chu S.T., Moss D.J., Morandotti R. *Opt. Express*, **22**, 6535 (2014).
9. Harris N.C., Grassani D., Simbula A., Pant M., Galli M., Baehr-Jones T., Hochberg M., Englund D., Bajoni D., Galland C. *Phys. Rev. X*, **4**, 041047 (2014).
10. Savanier M., Kumar R., Mookherjea S. *Opt. Express*, **24**, 3313 (2016).
11. Collins M.J., Xiong C., Rey I.H., Vo T.D., He J., Shahnia S., Reardon C., Krauss T.F., Steel M.J., Clark A.S., Eggleton B.J. *Nature Commun.*, **4**, 2582 (2013).
12. Helt L.G., Yang Z., Liscidini M., Sipe J.E. *Opt. Lett*., **35**, 3006 (2010).
13. Chen J., Levine Z.H., Fan J., Migdall A.L. *Opt. Express*, **19**, 1470 (2011).
14. Helt L.G., Liscidini M., Sipe J.E. *J. Opt. Soc. Am. B*, **29**, 2199 (2012).
15. Camacho R.M. *Opt. Express*, **20**, 21977 (2012).
16. Vernon Z., Sipe J.E. *Phys. Rev. A*, **92**, 033840 (2015).
17. Vernon Z., Sipe J.E. *Phys. Rev. A*, **91**, 053802 (2015).
18. Vernon Z., Liscidini M., Sipe J.E. *Opt. Lett*., **41**, 788 (2016).
19. Vernon Z., Menotti M., Tison C.C., Steidle J.A., Fanto M.L., Thomas P.M., Preble S.F., Smith A.M., Alsing P.M., Liscidini M., Sipe J.E. *Opt. Lett.*, **42**, 3638 (2017).
20. Garay-Palmett K., U'Ren A.B., Rangel-Rojo R. *Phys. Rev. A*, **82**, 043809 (2010).
21. Walls D.F., Milburn G.J. *Quantum Optics* (Berlin: Springer, 2008) p. 425.
22. Garay-Palmett K., Jerónimo-Moreno Y., U'Ren A.B. *Laser Phys.*, **23**, 015201 (2012).
23. Agrawal G.P. *Nonlinear Fiber Optics* (Amsterdam: Elsevier, 2007) p. 552.
24. Gondarenko A., Levy J.S., Lipson M. *Opt. Express*, **17**, 11366 (2009).
25. Krückel C.J., Fülöp A., Klintberg T., Bengtsson J., Andrekson P.A., Torres-Company V. *Opt. Express*, **23**, 25827 (2015).
26. Luke K., Okawachi Y., Lamont M.R.E., Gaeta A.L., Lipson M. *Opt. Lett.*, **40**, 4823 (2015).
27. Malitson I.H. *J. Opt. Soc. Am*., **55**, 1205 (1965).
28. Taillaert D., Van Laere F., Ayre M., Bogaerts W., Van Thourhout D., Bienstman P., Baets R. *Jpn. J. Appl. Phys.*, **45**, 6071 (2006).
29. Ikeda K., Saperstein R.E., Alic N., Fainman Y. *Opt. Express*, **16**, 12987 (2008).